

## Extended Use Of Spring Hammer Rapid Load Testing

K. Matsuzawa<sup>1</sup> and T. Matsumoto<sup>2</sup>

<sup>1</sup> International Association for Spring Hammer Rapid Load Test, Minato-ku, Tokyo, Japan,

<sup>2</sup> Graduate School of Natural Science and Technology, Kanazawa University, Kakuma-machi, Kanazawa, Japan

<sup>1</sup> E-mail: matsuzawa@po30.lcv.ne.jp

<sup>2</sup> E-mail: matsumot@t.kanazawa-uac.jp

**ABSTRACT:** Instruction As one of rapid load test methods, Spring Hammer test (SH test) method has been developed (Matsumoto et al., 2004) and used in practice. A simplified interpretation method of dynamic signals called Non-Linear Damping interpretation (NLD) is basically used for the SH rapid pile load test to derive a static response of the tested pile. In this paper, details of the Spring Hammer test method including NLD interpretation method is mentioned first. Second, validation of the SH test method is demonstrated through comparisons of static and the SH rapid load tests on relatively short piles and on circular rigid plates. Three case studies of the SH rapid load tests are then presented. The SH tests were conducted on perfect end-bearing piles (H-steel pile having end plate) in cases 1. In this SH tests, the NLD interpretation method did not work well to obtain the static behaviours of the piles due to the influence of wave propagation phenomena even though the pile lengths were relatively short compared to the loading durations. Hence, an extended NLD interpretation method is proposed for perfect end-bearing piles in case 1. In case 2, the SH test was carried out for estimating bearing characteristics of a pile group supporting a small bridge in service which was planned to be renewed, in order to make a decision whether existing pile foundations also were to be re-constructed or not. In case 3, the results of the SH plate load tests are compared with the static plate load tests on a saturated loam layer and on an improved soil. This paper discusses the applicability and limitation of the SH rapid load test methods through the case studies.

Keywords: Rapid load test, Bearing capacity, Wave propagation, Case study, Pile, Rigid plate

### 1. INTRODUCTION

It is widely believed that static load test (SLT) is the most reliable method to obtain load-settlement behaviour of a pile. However, the effect of interaction between the test pile and reaction piles should be considered to estimate a true load-settlement curve without the influence of the reaction system (Kitiyodom et al., 2004). In addition, static load test requires high cost and testing period. Therefore, pile design has been mainly based on empirical equation without SLT by adopting excessive design requirements, e.g. factor of safety of 3 in Japan.

In order to overcome the above situation, rapid load test methods have been proposed. As one of rapid load test methods, the Spring Hammer test (SH test) was proposed (Matsumoto et al., 2004). Loading mechanism of the SH test is basically similar to Dynatest (Gonin et al., 1984), Statnamic test (Birmingham et al., 1989) and Pseudo-static test (Schellingerhout et al., 1996). In the SH test method, the Non-Linear Damping (NLD) interpretation method (Matsumoto et al., 1994) is usually used to derive static load-settlement curve. Validity of the SH test, including NLD interpretation, has been confirmed through the comparative static and rapid load tests on piles and rigid plates (Matsuzawa et al., 2008a).

Pile testing is a fundamental part of pile foundation design. It is one of the more effective means of dealing with inevitable uncertainties that arise during the design and construction of piles (Poulos, 1998). Development and improvement of simple and convenient testing is expected to contribute to the design and construction control of foundations.

In this paper, first, typical SH test devices are introduced together with the testing method and the interpretation method. Then validity of the SH test method to estimate the static behaviour of a pile is examined through comparison of the results from SLTs and the SH tests. The application of the SH test to the rigid plate load testing is introduced as well.

In the latter part this paper, effective use of the SH test method are presented with three case histories. The first case is a topic on pile construction control. A piling method accompanying rapid load testing is introduced here. An extended use of simple interpretation enabled us to obtain static response of the perfect end bearing pile. The use of the SH test led to save of 60% of pile construction cost.

In the second case study, a loading test on an old bridge pier in service is presented. The SH test was used to examine the bearing capacity of a pile group supporting the bridge. The adoption of the SH test brought a great reduction of construction cost of foundation for the renewal works of the existing bridge.

In the third case study, the applicability of the SH test to the plate loading test on a loam and an improved soil is presented and discussed.

### 2. SPRING HAMMER TEST METHOD

#### 2.1 SH Rapid Load Test System

Several SH test devices are available, although their loading mechanism and measuring system are the same in the devices. Figure 1 shows the loading system and the measurement system of the SH test.

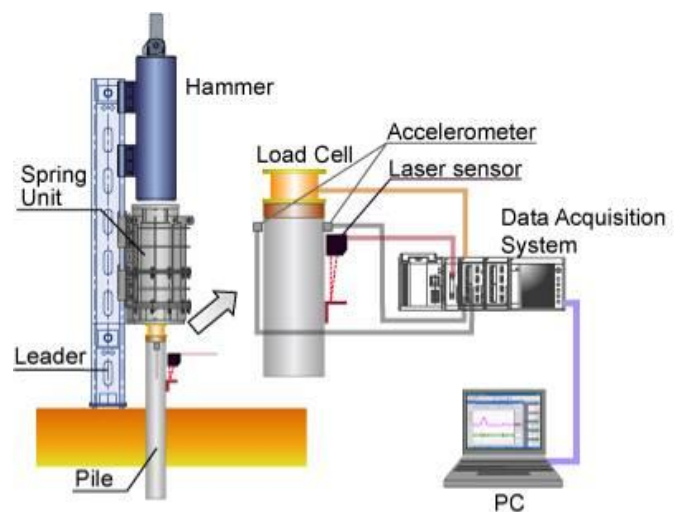


Figure 1 Loading system and measurement system

The loading system is composed of a leader, a spring unit and a falling hammer. Guide pipes mounted on the leader must prevent deviations of the central axis of pile, spring unit and falling hammer mass, ensuring verticality of their axes. Maximum load capacity is 2500 kN when using a hammer mass of 3 ton and a falling height of 3 m, which ensures confirmation of static pile capacity at least 2000 kN.

A load cell is placed on the pile top directly, on which the spring unit is placed. A hammer mass is dropped onto the spring unit to provide impact loading on the pile top. The acceleration at the pile top is measured using two accelerometers.

The pile top displacement is measured by means of a laser or an optical displacement transducer. The dynamic signals are sampled at a sampling frequency greater than 1 kHz. The output dynamic signals are recorded through a computerised data acquisition system. The recorded dynamic signals are promptly processed to derive 'static' response of the pile using the Non-Linear Damping method.

**2.2 SH Test Devices**

Figures 2, 3 and 4 show three types of the SH test devices; machine mounted, crawler carriage and portable tripod types. The spring unit for these devices consists of a number of coned disc springs.

The total spring stiffness of the spring unit is easily controlled by changing arrangement of the coned disc springs. The maximum load and loading duration can be widely varied by changing combination of the spring stiffness,  $k$ , the hammer mass,  $m_H$ , and the falling height of hammer,  $h$ . That is, basically, the loading duration can be prolonged by decreasing  $(k/m_H)^{0.5}$ , the maximum load can be increased by increasing  $(m_H k)^{0.5}$  or  $h^{0.5}$ . And, these values are affected also by the pile head stiffness of the tested pile. The nominal specifications of the currently available SH test devices are shown in Table 1 for cases where pile head stiffness is large enough. In principle, it is possible to manufacture SH devices that have much more larger loading capacities.

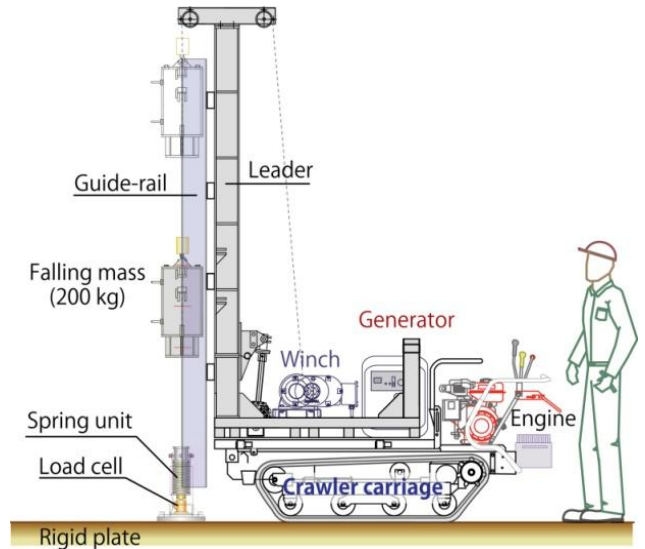


Figure 3 Crawler carriage type

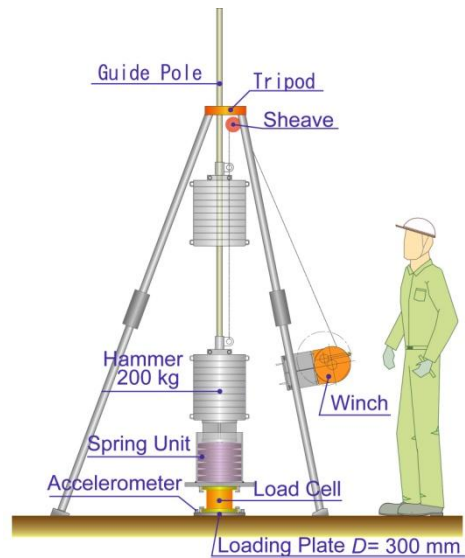


Figure 4 Tripod type SH test device

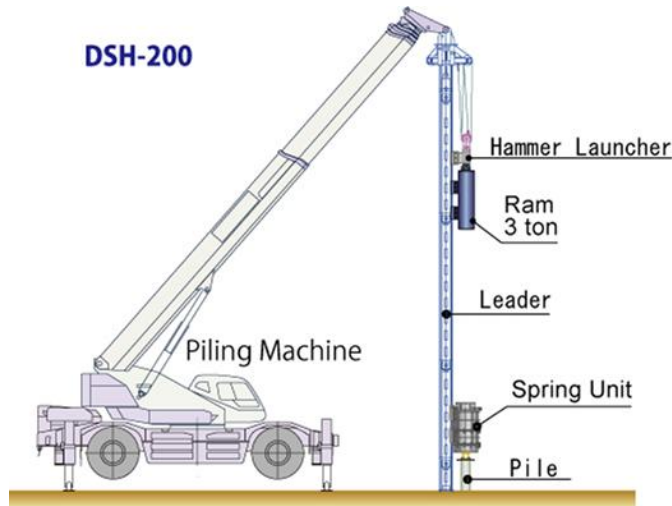


Figure 2 Machine-mounted SH test device

**Table 1 The SH test devices available**

	DSH-200	DSH-005C	DSH-005
Device type	Machine mounted	Crawler carriage	Tripod
Hammer mass (ton)	3	0.2	0.2
Max. fall height of hammer (m)	3	1.4	0.7
Spring stiffness (kN/m)	35000 (variable)	1250 (variable)	1250 (variable)
Max. load (kN)	2500	200	100
Weight of spring unit (kN)	25	0.5	0.5
Number of tests per day	5 to 7	8 to 10	8 to 10

Mobility and quick testing procedure is a primary advantage of the rapid load test. Photo 1 shows the SH test carried out in the yard of a railway station to investigate the bearing capacity of the ground for a new platform construction.

Due to the restriction of access of machineries, reaction system for SLT was not available. Furthermore, as shown in Photo 1, the railway was in service and trains were passing by the test location in intervals of 4 or 5 minutes. Vibrations due to the traffic of the trains disturbed the long term measurement of SLT.



Photo 1 SH testing in the railway station yard

The portable SH device was adopted to carry out the rigid plate load test in this location. The parts of the device were transported by man power, and the device was assembled at the test location. The SH plate load tests were carried out between passing of trains. The traffic did not disturb the measurement of the SH tests and the SH test did not interfere the traffic of trains.

The SH test carried out beside a railway bridge in service is shown in Photo 2 as well. In this site, H-steel piles having a length of 40 m were being constructed by a vibratory method while the SH tests were carried out. The SH test did not interfere the adjacent works in the construction site and could avoid delay of pile construction work.



Photo 2 SH test beside the railway bridge in service

### 2.3 Non-Linear Damping Interpretation Method

One of advantages of the rapid load test is that simplified interpretation methods, in which the pile is treated as a rigid mass neglecting wave propagation phenomena in the pile, could be used to derive a static load-displacement relation from the measured dynamic signals. In the SH test, Non-linear Damping interpretation (Matsumoto et al., 1994) is usually used to derive static response of the pile.

Figure 5 shows the modelling of pile and soil during rapid pile load testing. The pile is assumed as a rigid mass having mass of  $M_p$ , and the soil is modelled by a spring and a dashpot in parallel. This modelling has been advocated by Middendorp et al. (1992) and Kusakabe & Matsumoto (1995).

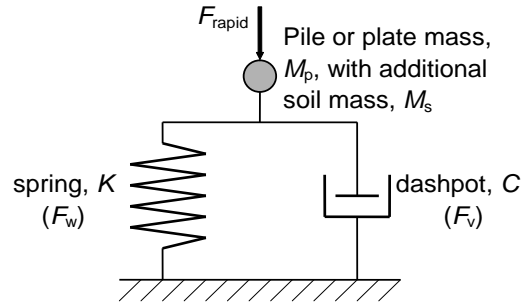


Figure 5 Modelling of Rapid Load Test

The additional soil mass beneath the pile or plate,  $M_s$ , can be estimated as follows following Randolph and Deeks (1992):

$$M_s = 2D^3 \frac{0.1 - \nu^4}{(1 - \nu)} \rho_s \quad (1)$$

where  $\nu$  and  $\rho_s$  are Poisson's ratio and density of the soil, and  $D$  is the plate diameter.

Figures 6 and 7 show the notations used in the Non-Linear Damping method. The applied load,  $F_{\text{rapid}}$ , is equal to the sum of the soil resistance,  $F_{\text{soil}}$ , and the inertias of the pile mass and the additional soil mass:

$$\begin{aligned} F_{\text{soil}}(i) &= F_{\text{rapid}}(i) - (M_p + M_s) \cdot \alpha(i) \\ &= F_{\text{rapid}}(i) - M \cdot \alpha(i) \end{aligned} \quad (2)$$

where  $M$  is the sum of the pile or plate mass and the additional soil mass, and  $\alpha(i)$  is the measured pile acceleration at time step  $i$ .

The soil resistance,  $F_{\text{soil}}$ , is the sum of the spring resistance (static resistance),  $F_w$ , and the dashpot resistance (velocity dependent resistance),  $F_v$ .

$$F_{\text{soil}}(i) = F_w(i) + F_v(i) = F_w(i) + C(i) \cdot v(i) \quad (3)$$

where  $C(i)$  is the damping factor and  $v(i)$  is the pile velocity at time step  $i$ .

At the first step ( $i = 1$ ), the initial stiffness,  $K(1)$ , is calculated as the initial static load,  $F_w(1)$ , divided by the initial displacement,  $w(1)$ .

$$K(1) = F_w(1)/w(1) = F_{\text{static}}/w_{\text{static}} \quad (4)$$

At the next step (at step  $i+1$ ), the soil spring,  $K(i+1)$  is assumed to be equal to  $K(i)$  as indicated by Eq. (5). Hence, the static resistance,  $F_w(i+1)$ , at step  $i+1$  is calculated by Eq. (6). The value of  $C(i+1)$  can be determined by means of Eq. (7).

$$K(i+1) = K(i) \quad (5)$$

$$F_w(i+1) = F_w(i) + K(i+1) \cdot \{w(i+1) - w(i)\} \quad (6)$$

$$C(i+1) = \{F_{\text{soil}}(i+1) - F_w(i+1)\} / v(i+1) \quad (7)$$

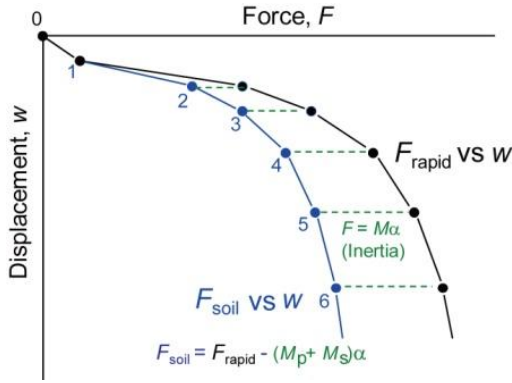


Figure 6 Correction of inertia to obtain soil resistance

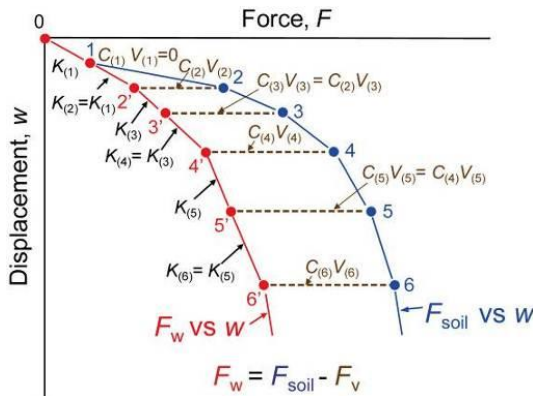


Figure 7 Non-linear damping interpretation

At the following step  $i+2$ ,  $C(i+2)$  is assumed to be equal to  $C(i+1)$  as indicated by Eq. (8). Therefore, the values of  $F_w(i+2)$  and  $K(i+2)$  can be determined by means of Eqs. (9) and (10), respectively.

$$C(i+2) = C(i+1) \tag{8}$$

$$F_w(i+2) = F_{soil}(i+2) - C(i+2) \cdot v(i+2) \tag{9}$$

$$K(i+2) = \frac{F_w(i+2) - F_w(i+1)}{w(i+2) - w(i+1)} \tag{10}$$

By repeating the procedure from Eq. (5) to Eq. (10), the values of  $K$  and  $C$  for following steps are alternately updated consecutively. Finally, the whole static load-displacement relation,  $F_w$  vs  $w$ , is constructed as shown in Fig. 7.

The authors are aware that various methods have been proposed for interpretation of rapid load test signals. For examples, Mullins et al. (2002) proposed the Segmental Unloading Point method for interpreting the rapid load test signals of longer piles, Lin et al. (2004a) extended the structural damping concept (Lin et al., 2004b) to accommodate longer piles, in which displacement related soil damping is used in the segmental method. Stokes et al. (2008) discussed non-linear (non-constant) soil damping to be used in interpretation of rapid load test signals of piles. However, in this paper, rapid load test signals are basically interpreted using the above-mentioned Non-Linear Damping (NLD) method proposed by Matsumoto et al. (1994) to derive static response of piles or rigid plates, because the NLD method utilises the measured signals (applied force, acceleration, velocity and displacement at the pile

head) alone. It is very easy to derive the static response of pile or rigid plate promptly at test site using the NLD method.

### 3. VALIDATION OF SH TEST METHOD

#### 3.1 Comparative Test on Steel H-Piles

In order to confirm the validity of the SH test method, both the static and the SH rapid load tests were carried out on steel H-piles (Matsuzawa et al, 2008a).

Figure 8 shows the profiles of soil layers and SPT N-values at the site, together with installed seven H-shaped steel piles (300 mm x 300 mm). These piles had an end plate at the pile toe so that large end bearing capacity was expected. Each pile was installed by means of bored construction method using cement slurry around the pile. The pile was finally driven after inserting the pile into the pre-bored hole. Piles No. 1 and No. 3 were subjected to the static load test after a curing period of 7 days from the end of the pile installation. The SH tests were carried out immediately after the completion of the static load test of each pile.

Figure 9 shows examples of dynamic signals from rapid load test on pile No. 3 having a length of 3 m. The pile head velocity was obtained by integration of the measured acceleration with respect to time. The pile head displacement was measured using an optical displacement transducer. The loading duration was 100 ms that corresponded to the relative loading duration  $T_r = t_L / (2L/c) = 85$ , where  $t_L$  is the loading duration and  $c$  is wave propagation speed in the pile ( $c = 5100$  m/s). In the Method for Rapid Load Test of Single Piles by Japanese Geotechnical Society (JGS, 2002), load test with  $T_r$  greater than 5 is regarded as rapid loading, where wave propagation phenomena in the pile can be neglected.

Figure 10 shows the static load-displacement curve,  $F_w$  vs  $w$ , derived using the NLD interpretation method, together with  $F_{rapid}$  vs  $w$  and  $F_{soil}$  vs  $w$ .

Figure 11 shows the changes in values of  $K$  and  $C$  with pile head displacement. The value of  $K$  decreases rapidly with increasing the pile head displacement and becomes almost zero at pile head displacement of 32 mm. The value of  $C$  also decreases rapidly until the pile head displacement attains about 10 mm, and levels off after that. It is thought that the decrease in  $C$  value reflects decrease in the radiation damping due to the progressive slip failure at the pile shaft. It is also thought that the residual value of  $C$  around 20 kNs/m reflects the viscous damping.

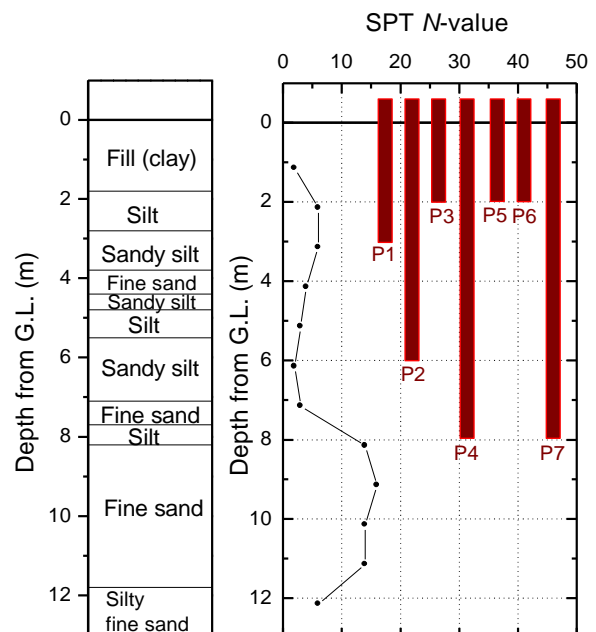


Figure 8 Profiles of soil layer and SPT N-values

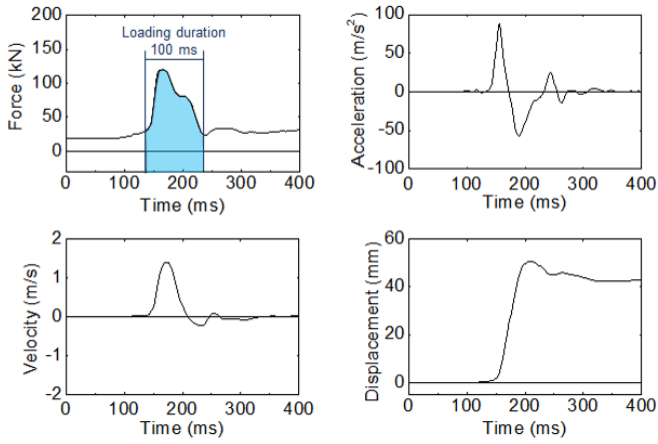
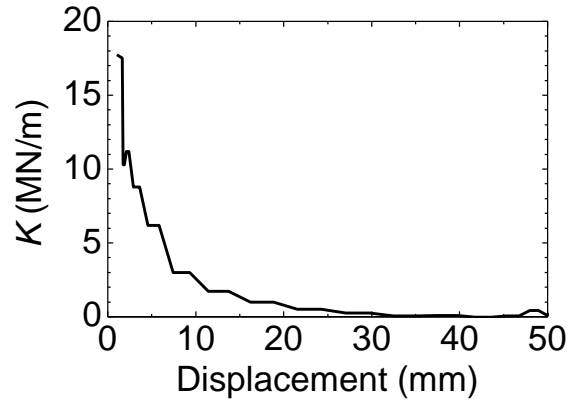


Figure 9 Measured test signals on pile No. 3



(a) Change of K value

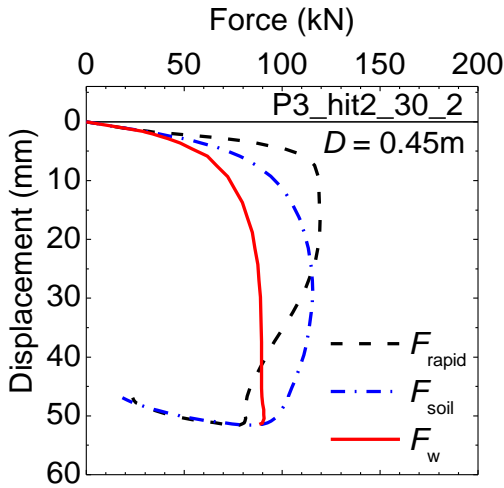
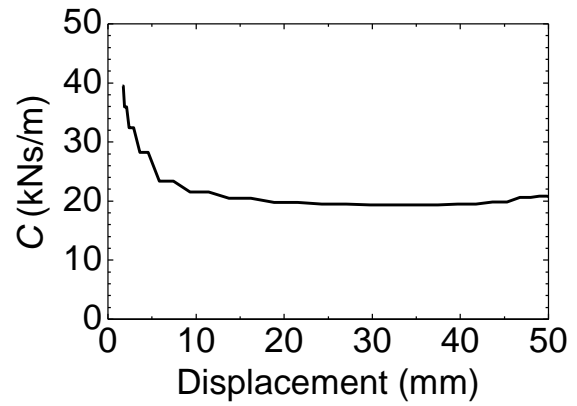


Figure 10 Static load-displacement relations of pile No. 3 from the Non-Linear Damping interpretation



(b) Change of C

Figure 11 Changes in K and C with pile head displacement

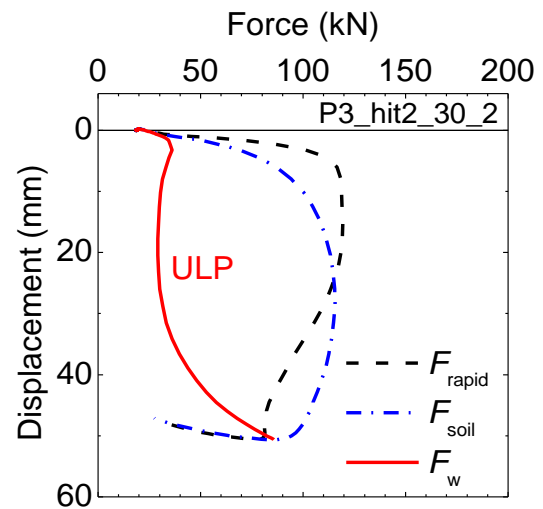


Figure 12 Static Load-Displacement Relations of Pile No.3 after the Unloading Point (ULP) method

Figure 12 shows the static response derived using the unloading point method (ULP) proposed by Kusakabe & Matsumoto (1995) on the same hammer blow as Fig. 10. In the ULP method, dashpot coefficient,  $C$ , is treated as constant through the loading. On the other hand, both of soil spring,  $K$ , and  $C$  are treated as non-linear in the Non-Linear Damping interpretation.

Figure 13 shows the comparison of static load-displacement relations of pile No. 3 obtained from the static load test and the SH rapid load test with the NLD interpretation. The vertical axis of the figure denotes the accumulated pile head displacement. It can be seen from the figure that the envelope of the curves from the static load test and the rapid load tests is consistent, regardless of drop heights of the hammer used in the SH tests. The envelope was drawn manually. It is clearly seen that the static curve derived using the ULP method (Fig. 12) is not comparative to the SLT result.

Similar comparison was made also for pile No. 1 having a length of 4 m, as shown in Fig. 14. The envelope of the curves from both test methods is consistent again.

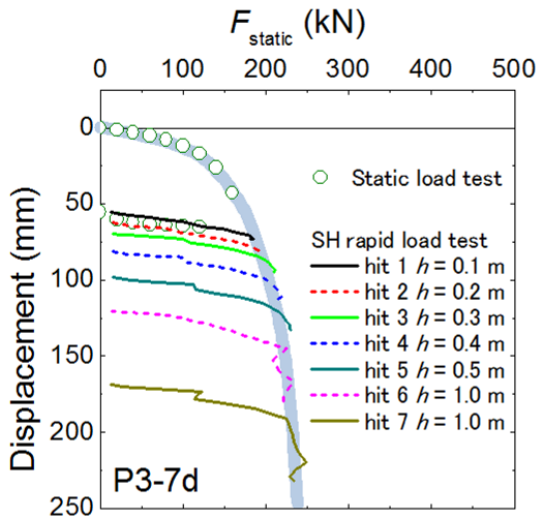


Figure 13 Load-displacement relations from static and consecutive rapid load tests on pile No. 3

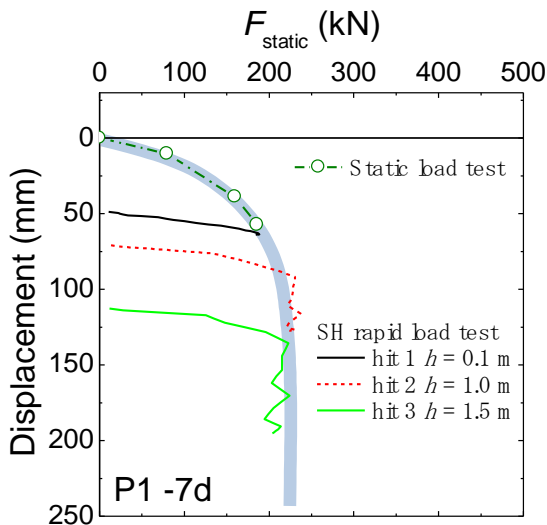


Figure 14 Comparison of load-displacement relations from static and consecutive rapid load tests on pile No. 1

### 3.2 Comparison of Rapid and Static Plate Loading Tests

In order to investigate the applicability of the SH rapid load test to rigid plate load testing, a series of comparative static and rapid load tests on rigid plates were carried out.

The test site was located at the east coast of Tokyo bay. The tests were carried out at 6 locations on the site, as shown in Fig. 15. The surface fill layer consisted of fine sand containing fist-sized gravels. The soil consists of 4.3% of gravel, 52.1% of sand, 32.9% of silt and 10.7% of clay. To avoid probable obstacles, the ground surface was excavated to a depth of 0.5 m to create a test pit.

A rigid plate with a diameter of 0.3 m was used throughout in the tests. For plate No. 1, the rapid load test using the SH device was conducted first, followed by the static plate load test. In contrast, in plate No. 2, the static load test was performed first, followed by the rapid load tests. A truck containing steel plates, 80 kN in total, was used for the reaction weight in the static load tests, as shown in Photo 3.

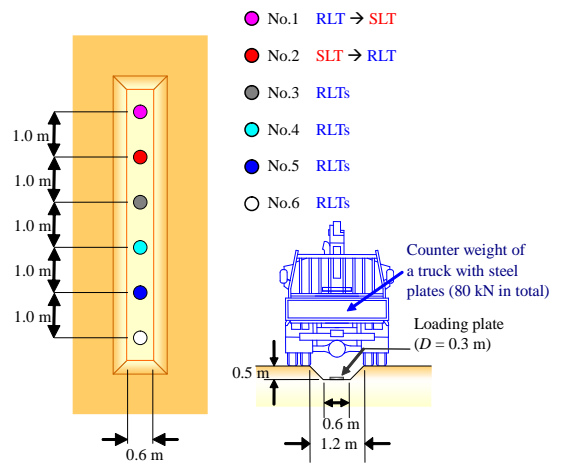


Figure 15 Locations of test plates and test pit profiles



Photo 3 Static plate load test on Plate No.1

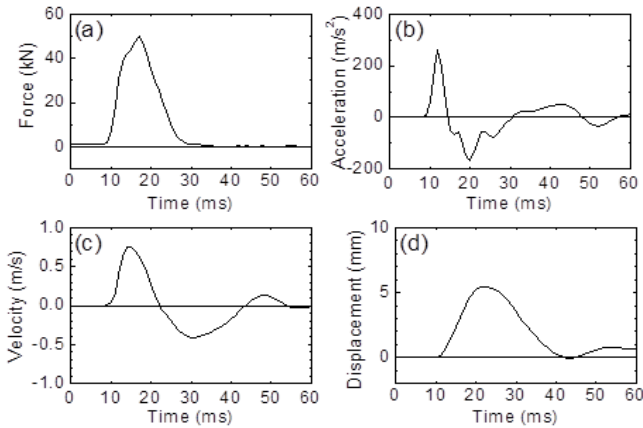


Figure 16 Examples of measured signals from rapid plate load test, (a) Force applied onto the plate, (b) Acceleration, (c) Velocity, (d) Displacement

Examples of test signals obtained from a rapid plate load test are shown in Fig. 16. The velocity and displacement of the plate were obtained from single and double integrations of the measured acceleration with respect to time, respectively.

Loading duration was about 25 ms which was shorter compared to that in the rapid pile load test, and the maximum acceleration exceeded 300 m/s<sup>2</sup> which was greater than that in the rapid pile load test (see Fig. 9).

Figure 17 shows the load-displacement behaviour of plate No. 1 obtained from the SH tests. All the curves are the static behaviours derived using the non-linear damping interpretation. The static load tests were carried out between the 2nd and 3rd rapid load tests.

Figure 18 compares all the load-displacement relations obtained from the static test and the rapid tests. The settlement in each test is zeroed for comparison. It can be seen from the figure that the initial stiffness from the static test and the rapid tests are almost equal.

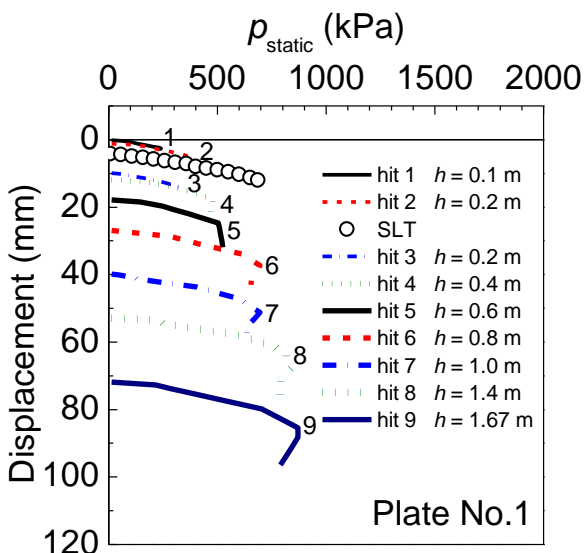


Figure 17 Results of rapid plate load tests on Plate No.1

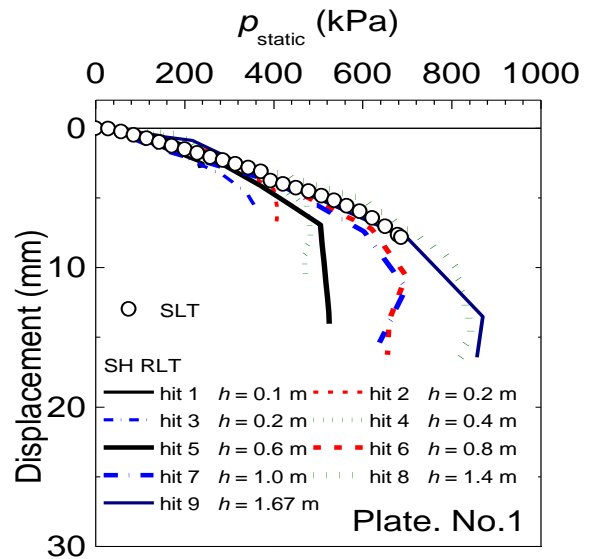


Figure 18 Results of rapid plate load tests and SLT on plate No.1 (initial settlement zeroed)

Similar comparative tests were carried out for plate No. 2. Fig. 19 shows the comparison of the test results. Static load tests were performed twice before the consecutive SH rapid tests. Maintained loading (30 min loading duration in each load step) was adopted in the first static load test, while continuous loading was adopted in the second static test where the pressure,  $p$ , was increased to 900 kPa in 20 min without holding the load. Further loading was not possible because of the limit of the reaction weight.

The initial stiffness in the second static test was almost equal to that of the unloading curve in the first static test. The curves obtained from the SH rapid tests show good agreements with the previous static test results. The envelope of the all the curves from the static and rapid tests is indicated by the heavy line in the figure. It is seen that the envelope of the curves from both test methods is consistent.

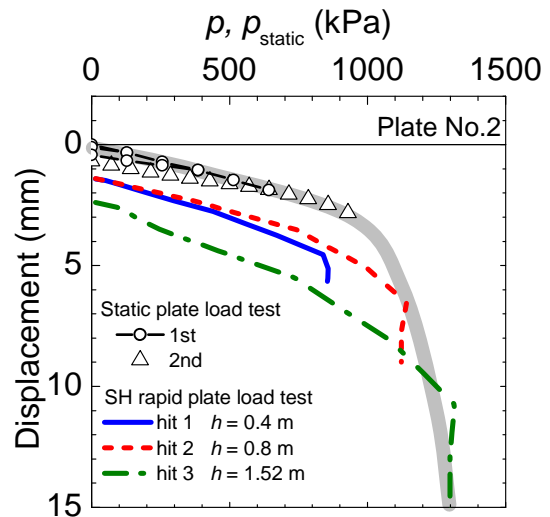


Figure 19 Results of rapid and static plate load tests on plate No.2

**4. CASE 1: CONSTRUCTION CONTROL OF BEARING PILES**

**4.1 Piles Construction**

A temporary platform structure was planned in Saitama, Japan (Matsuzawa et al., 2008b). Fig. 20 shows the profiles of soil layers and SPT *N*-values in the building construction site. The piles were H-steel piles (350 x 350 mm) with a circular end plate of *D* = 0.54 m.

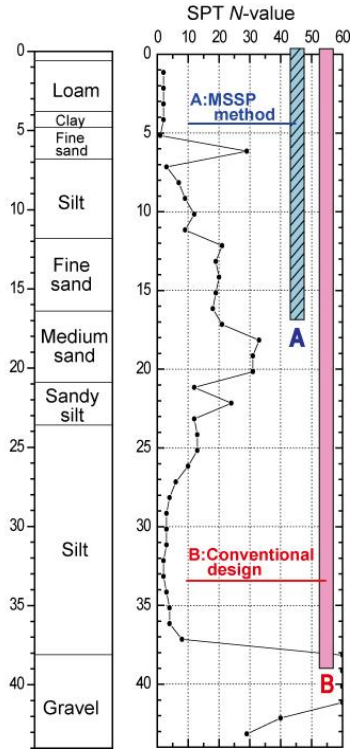


Figure 20 Profiles of soil layer and SPT *N*-values in building construction site in Saitama

The design load on the piles was 783 kN. A factor of safety of 1.5 was adopted. Hence the required ultimate pile capacity was 1175 kN. It is common practice in Japan that the pile toe is penetrated in a soil layer having *N*-value greater than 50 in cases of temporary piles. In this preliminary design, the pile length was 39 m so that the pile toe reached the hard gravel layer.

If an empirical pile design equation (11) specified in Structural Design and Construction Manual for Temporary Buildings and Structures (AIJ, 1994) is adopted, the end bearing capacity of the pile having *L* = 39 m is 2121 kN and the shaft capacity is 6522 kN giving the total capacity of 8643 kN in this site.

$$Q = Q_b + Q_s = 150 N_p A_p + U \sum \alpha N_i l_i \quad (\text{kN}) \quad (11)$$

where *Q<sub>b</sub>* = the end capacity, *Q<sub>s</sub>* = the shaft capacity, *N<sub>i</sub>* = SPT *N*-value in soil layer *i*, *A<sub>p</sub>* = cross-sectional area of the end plate (m<sup>2</sup>), *l<sub>i</sub>* = length of soil layer *i* (m), *U* = circumferential length of the pile (m),  $\alpha = 2$  for sand and 20 for clay.

The bearing capacity of the pile with *L* = 39 m seemed to be excessively overdesign. Hence the pile length was reduced to 17 m from 39 m in the second design stage. The end capacity and the shaft capacity of the pile with *L* = 17 m were estimated to be 653 kN and 958 kN respectively, resulting in the total capacity of 1611 kN.

The piles were constructed by means of bored and driven method. The piling procedure is as shown in Fig. 21. Cement slurry was poured into the borehole to gain the shaft resistance. The SH rapid load test is carried out just after the pile installation before the

cement slurry hardens to measure the end resistance. This piling method is called MSSP.

Prior to the final decision of the pile length, the SH rapid load tests were conducted on 5 test piles having *L* = 17 m to confirm the validity of the second design.

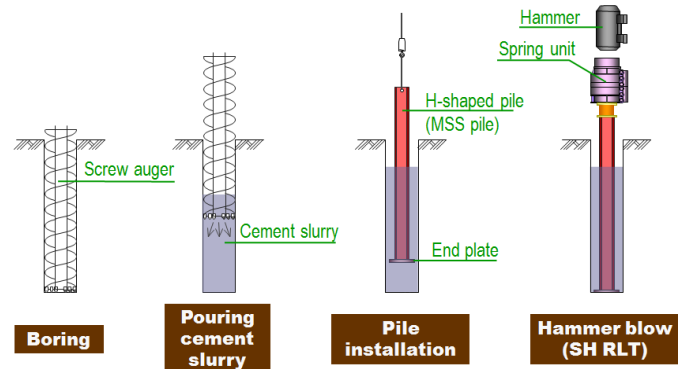


Figure 21 Pile construction procedure of MSSP method

**4.2 Dynamic Signals of Perfect End-Bearing Pile**

Figure 22 shows examples of dynamic signals from the SH rapid load test on pile No. 10 at the time of pile installation: (a) pile head force, (b) acceleration, (c) velocity and (d) displacement. The pile head velocity was obtained by integration of the measured acceleration with respect to time. The pile head displacement was obtained by double time integration of the measured acceleration.

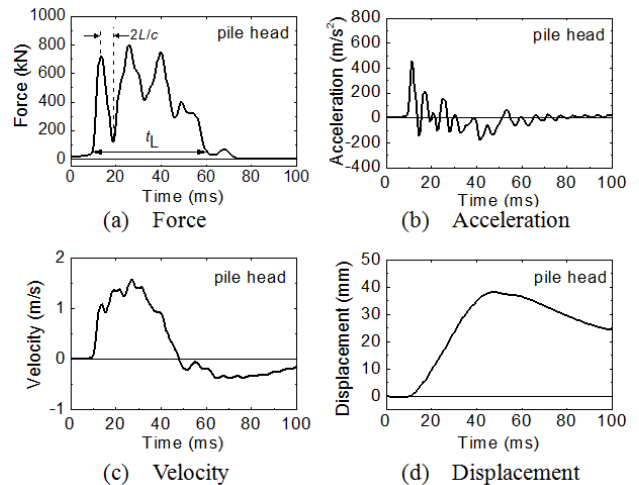


Figure 22 Examples of measured dynamic signals

The loading duration, *t<sub>L</sub>*, was 50 ms that corresponded to the relative loading duration  $T_r = t_L / (2L/c) = 7.5$ . It is seen from Fig. 22(a), however, that the pile head force and acceleration fluctuate with an interval of 6.7 ms that corresponds to the return travelling time of a wave in the pile ( $2L/c$ , *c* = 5100 m/s).

As mentioned earlier, the MSS pile is H-shaped steel pile having a uniform cross-section with a circular plate at the lower end of the H-steel, and the shaft resistance is negligible at the time of installation. Hence, the influence of wave propagation in the pile cannot be neglected, even if *T<sub>r</sub>* is greater than 5.

**4.3 Extended Non-Linear Damping Interpretation Method**

In order to cope with the above-mentioned situation, the Non-linear Damping interpretation is used along with the one-dimensional wave propagation theory. In this interpretation method, wave propagation in the H-steel pile is taken into account, while the end plate and the additional soil beneath the plate are still treated as one mass,  $M$ .

The idea is that force on the end plate is obtained using Eqs. (12), (13) and (14), on the basis of the characteristics solutions of the wave equation (see Fig. 23). This idea is the same as that used in CASE method proposed by Raushe et al (1985).

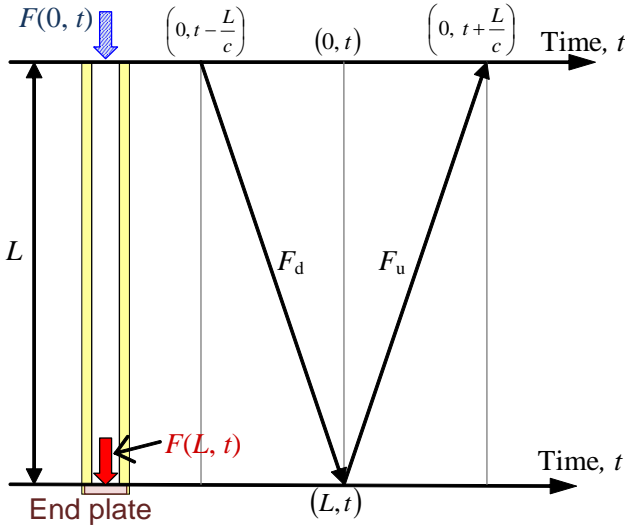


Figure 23 Wave propagation in a perfect end-bearing pile

$$F_d(0, t) = \{F(0, t) + Z \cdot v(0, t)\} / 2 \tag{12}$$

$$F_u(0, t) = \{F(0, t) - Z \cdot v(0, t)\} / 2 \tag{13}$$

where  $F_d$  and  $F_u$  are downward and upward travelling forces at the pile head respectively,  $F$  and  $v$  are force and velocity measured at the pile head, and  $Z$  is mechanical impedance of the pile.

$$F(L, t) = F_d\left(0, t - \frac{L}{c}\right) + F_u\left(0, t + \frac{L}{c}\right) \tag{14}$$

$$v(L, t) = \frac{1}{Z} \left\{ F_d\left(0, t - \frac{L}{c}\right) - F_u\left(0, t + \frac{L}{c}\right) \right\} \tag{15}$$

$$\alpha(L, t) = \frac{\partial v(L, t)}{\partial t} \tag{16}$$

$$w(L, t) = \int v(L, t) dt \tag{17}$$

The velocity,  $v$ , acceleration,  $\alpha$ , and displacement,  $w$ , at the lower end of H-steel are estimated by means of Eqs. (15), (16) and (17), respectively.

The Non-linear Damping interpretation analysis is carried out using thus obtained dynamic signals on the end plate. This interpretation procedure is called the ‘Extended Non-linear Damping method’.

Figure 24 shows the estimated force, acceleration, velocity and displacement on the end plate, compared with those measured at the pile head. It can be seen from Fig. 24(a) that the force on the end plate (= force at the pile tip) no longer fluctuate.

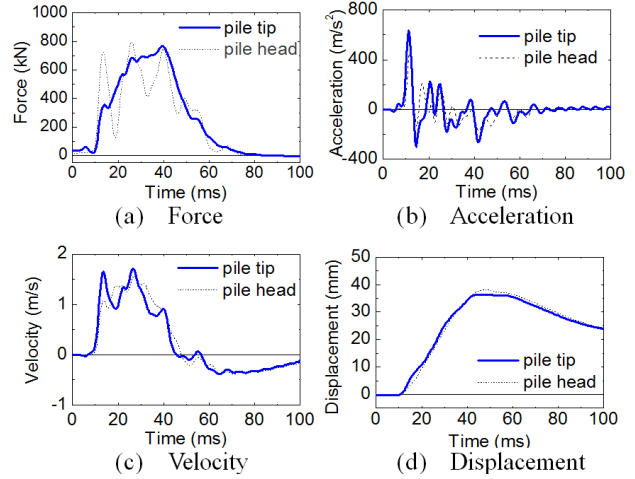


Figure 24 Dynamic signals on the end plate converted from the signals at the pile head

Figure 25 shows the force on the end plate vs plate displacement and the pile head force vs pile head displacement. The non-linear damping analysis was conducted using the force on the end plate as  $F_{rapid}$ . The results of the Non-Linear Damping analysis are shown in Fig. 26.

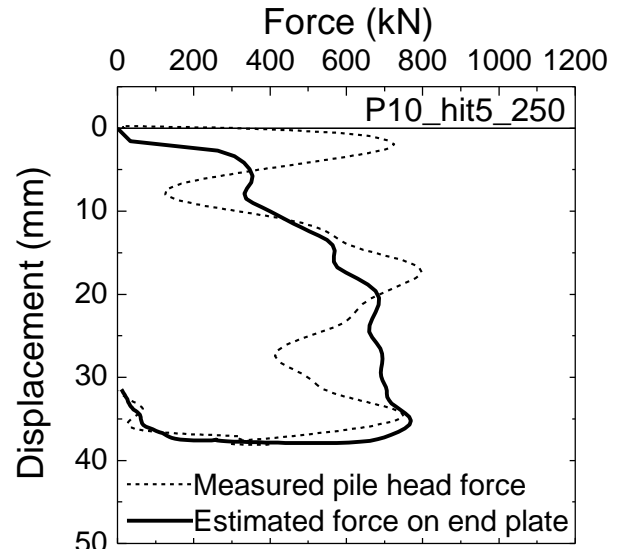


Figure 25 Measured and converted force-displacement relations

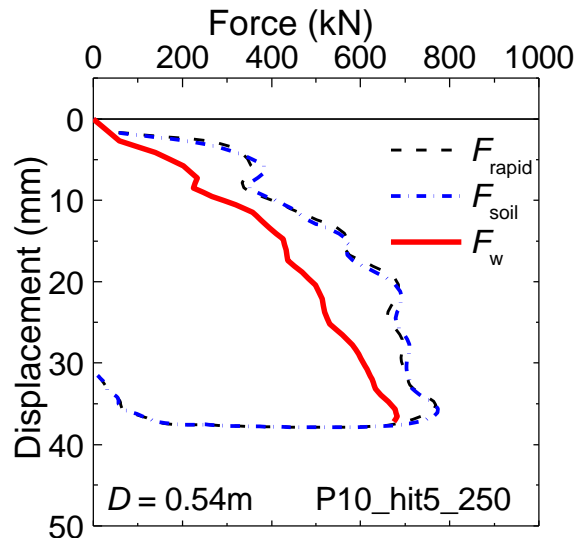


Figure 26 Example of results of extended NLD

4.4 SH Test Result

Figure 27 shows the results of the SH tests on all the piles. The static load-displacement curves of the 5 test piles from the SH tests are shown by the red dashed lines in Fig. 27. Since the SH tests were carried out 1 day curing period after the pile installation process, the test piles had the shaft resistance as well as the toe resistance. In the SH tests on these piles, they had no permanent (residual) settlements. The confirmed pile resistance was larger than the required value of 1175 kN with a very small pile head displacements less than 2 mm. Based on these test results, the pile length was determined as 17 m.

A total of 27 piles were constructed in this site. For the purpose of construction control, the SH tests were carried out on all the constructed piles at the end of pile installation process when the shaft resistance could not be expected. In these construction control tests, the shaft resistance was estimated from Eq. (11), reducing the calculated value by a factor of 0.8 for a safe side estimation. Thus estimated shaft resistance was 766 kN. Hence, confirmation of the toe resistance exceeding 409 kN was the construction control criteria.

It can be seen from the figure that all the piles had the toe resistance greater than 409 kN. Note here that the allowable pile head displacement was 30 mm.

As a consequence of adopting construction control using the SH test, pile construction cost was reduced to 60% of that in the conventional design.



Photo 4 SH devices placed on the bridge

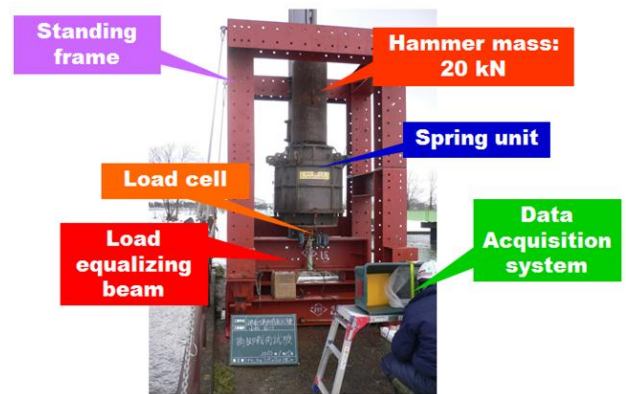


Photo 5 SH devices set in the framework structure

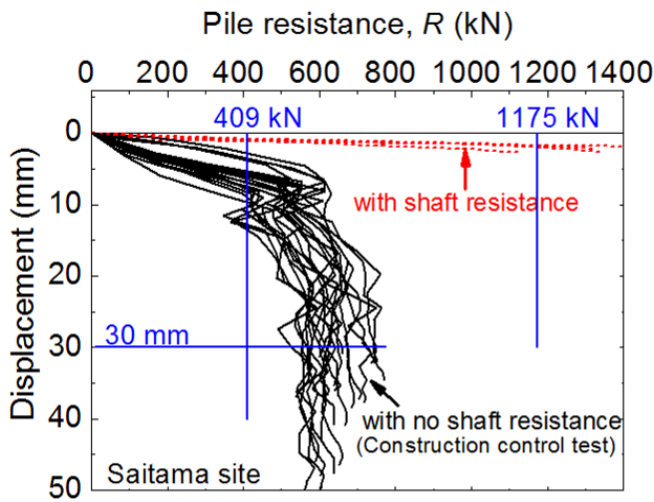


Figure 27 Load-displacement relations of all piles

5. CASE 2 : SH TEST ON PILE GROUP FOUNDATION FOR A BRIDGE IN SERVICE

5.1 Test Description

A renewal project of an old bridge was planned. The bridge is used for pedestrians and light-weight vehicles. It has a width of 2.4 m and a total span length of 80 m, with 2 abutments and 7 piers. Each pier consists of 3 RC piles having a diameter of 0.4 m, a length of 12.2 m (1.8 m above bundle, bundle of 0.4 m, 10 m below bundle) and a centre-to-centre pile spacing of 1.0 m. The objective of the SH test was to confirm that the pile foundations have the required bearing capacity of 300 kN in order to make a judgement whether the foundation should be reconstructed or not for the renewal of the bridge.

The SH load tests were carried out on the floor deck just above one of the piers. Photo 4 shows the SH test device used. It was placed on the floor deck just above the centre of the test pier. In order to load equally on 3 piles, a load equalizing beam was prepared as shown in Photo 5.

Figure 28 shows the alignment of measuring instruments used in this test. Applied rapid load was measured by a load cell placed on the load equalizing beam. Two strain gauges were mounted on each pile to measure the axial force of each pile. Displacement of the pile group was calculated by double integration of accelerations measured by four accelerometers (A) attached on the bundle of the piles. Accelerometers (B) were attached on pile 2 to obtain the longitudinal wave propagation velocity of the pile material.

The SH tests were carried out with four steps of loading, with increasing of falling height of the hammer,  $h = 0.05, 0.15, 0.30$  and  $0.50$  m, with checking out the bridge condition after each blow.

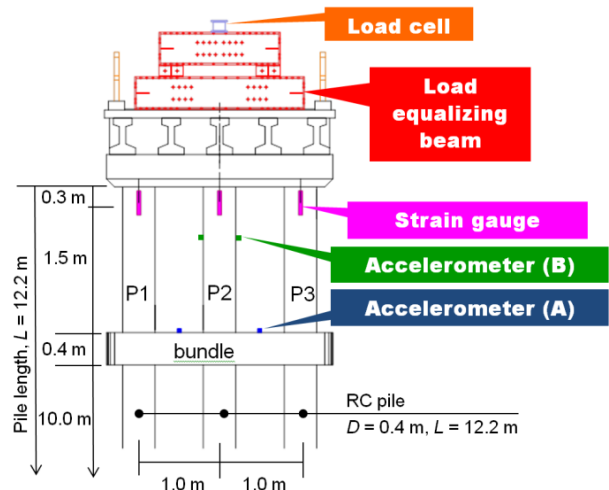


Figure 28 Alignment of measuring instruments

5.2 SH Test Results

Figure 29 shows the dynamic signals of the applied load on the floor deck measured by the load cell (LC) and the axial forces of each pile calculated from measured strain of the piles with respect to the time in the SH test with  $h = 0.5$  m. The longitudinal wave propagation speed,  $c$ , of the pile was estimated to be 3000 m/s from the measurements of the accelerations at A and B. Young's modulus,  $E$ , of the pile material was estimated as  $2.16 \times 10^7$  kPa using the relation of  $E = \rho c^2$  where  $\rho$  is the density of the pile of  $2.4 \text{ t/m}^3$ . Axial force,  $F$ , of each pile was calculated using thus estimated Young's modulus,  $E$ , the measured strain,  $\epsilon$ , and the cross-sectional area of the pile,  $A$ , i.e.  $F = E\epsilon A$ . Peak values of the applied load on the floor deck and sum of axial forces of the piles were 319 kN and 280 kN, respectively. The total axial force of the piles was reduced to only 88% of the applied load. This was due to that the bridge girders were simple beams. The NLD interpretation method was adopted using the total pile force as input rapid force to derive the static response of the pile group. In this case, the loading duration,  $t_L$ , was 45 ms and the relative loading duration of this test was  $T_r = t_L/(2L/c) = 7.6$ , where  $L = 11.9$  m (pie length below the strain measurement) and  $c = 3000$  m/s.

Figure 30 shows the measured rapid load vs displacement curves from the SH tests. Note that no residual settlement was observed in the SH tests.

Figure 31 shows the derived static response of the pile group. While a little fluctuations are seen in the curves, the response of the pier is linear behaviour during a series of the SH tests. The test results show that the settlement of the pier is less than 1 mm when a load of 430 kN is applied.

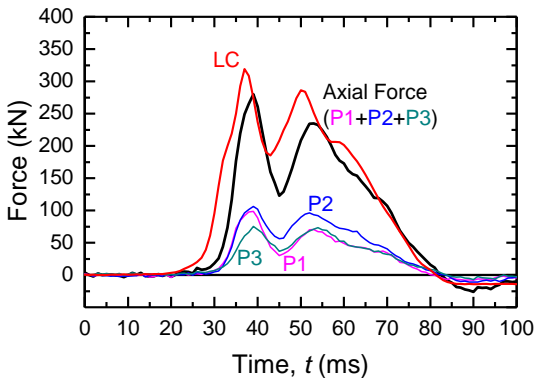


Figure 29 Applied load and axial force of each pile

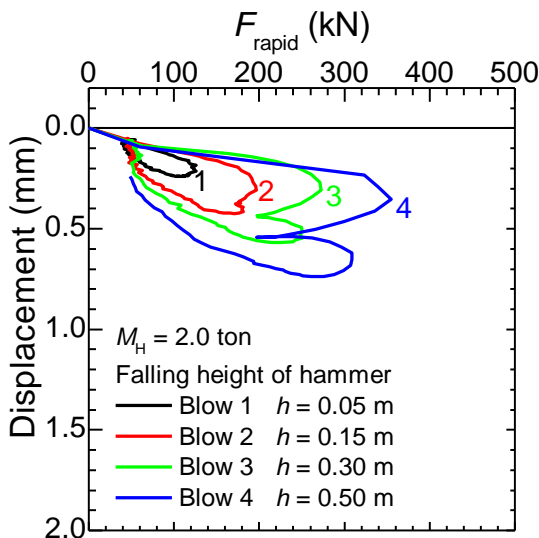


Figure 30 Load (rapid) - displacement curves

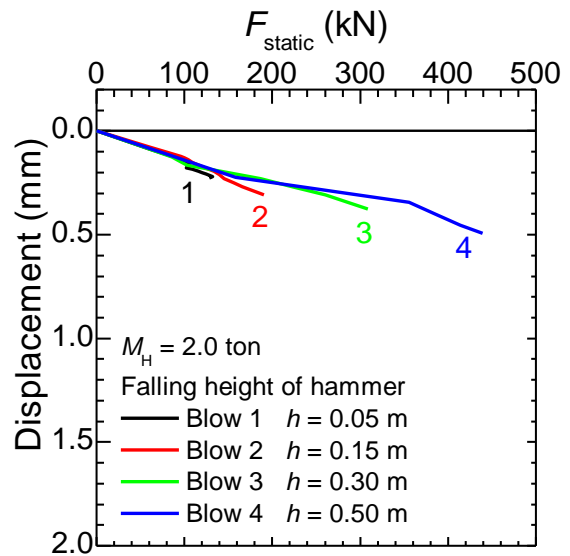


Figure 31 Derived static response of the bridge pier

It was judged from the SH test results that the existing piers have the required bearing capacity resulting in minor repair work of the deck plates. That is, the SH tests on the old bridge brought a large reduction of cost for reconstruction of the bridge foundation. The closure of the traffic on this bridge for the SH tests was only one working day.

6. CASE 3 : APPLICABILITY OF SH PLATE LOAD TEST

Plate loading test has been widely used in Japan to investigate bearing capacity of the ground including improved soils, road embankments and slope embankments. The static plate load tests are also used for design of raft foundations for buildings.

Although the static test is the most reliable method, it has been often avoided because of its inconvenience due to the long term measurement which interferes the other works in the site. Or even in case that the SLT is adopted, it is carried out on one or two locations usually at most in a wide construction area. It is important to investigate bearing characteristics densely in a construction area to decrease uncertainties or risks due to variations over the site.

As mentioned previously (see Comparison of Rapid and Static Plate Loading Tests), the SH plate loading test is applicable to the rigid plate load test on sandy ground. However, the test is not always simply applicable to any type of soil. In this chapter, the applicability of SH plate load tests to other types of soil, i.e. loam ground and improved soil, is presented and discussed.

6.1 Plate Load Test on Loam Ground

Heavy construction machines, pile driver, crane and etc., are necessary for construction works. It is a primary respect to keep safety works of these machines without any accident.

A working area for a pile driver was levelly created by excavation in the construction site for Tokyo Gaikan Highway. A surface soil was a loam layer, and the decrease of bearing capacity due to the earth work for preparation of the working area was apprehended. Hence, the SH test was adopted to confirm the bearing capacity of the ground for installation of the pile driving machine.

The maximum contact pressure of the machine was 100 kPa. It was required to confirm the bearing capacity greater than 200 kPa, twice of design load for short term capacity with a factor of safety of 2. The SH tests were performed at three locations in this site. The

static plate load test also was carried out at one of the SH plate load test locations.

The SLT was carried out with a maximum load of 120 kPa, 2 steps of loading, prior to the SH test on plate No.1. The loading and unloading rate was 2 kPa per second and the load was held for 30 min for virgin loading steps and 5 min for re-loading and unloading steps, following the Standards of Rigid Plate Test (JGS, 2003).

On the same plate, the SH test was carried out immediately after the SLT. In the SH test, three blows of the hammer were performed with falling heights of 0.1, 0.2 and 0.4 m.

Figure 32 shows the pressure (load divided by cross-sectional area of the plate) - displacement curves obtained from the SLT and the first blow of the SH test with the NLD interpretation. The residual settlement of the plate at the end of the SLT was 0.36 mm. In the SLT, displacement increased while the load was held for 30 min in each loading step due to consolidation and/or creep. It is seen from the figure that the increments of displacement in the SH test are smaller than those at the end of load holding in each loading step in the SLT. As we all know, it is difficult to obtain the static load-displacement relation of the rigid plate which contains displacement due to consolidation and/or creep. However, if we disregard increments of displacement due to consolidation and/or creep during load holding durations in the SLT, thus constructed load-displacement curve is almost the same as that derived from the SH test.

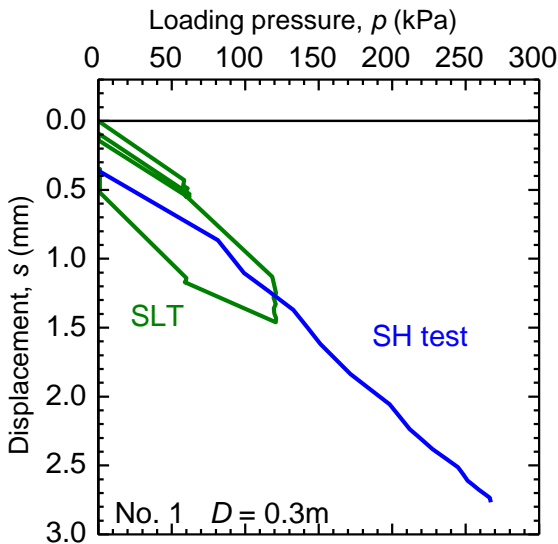


Figure 32 Load-displacement curves from SLT and SH test

In order to avoid underestimation of displacements derived from the SH tests, it was decided to use an empirical factor for the displacements in the SH tests from the comparison of the static test results and the curve derived from the first SH test. The pressure - displacement curve derived from the SH in which the displacement was multiplied by a factor of 1.4 is shown in Fig. 33, together with the static test results measured at the end of each load holding. The factored curve is comparable with the static test results. Hence, it was decided to use the factor of 1.4 for the displacements measured in the SH tests in this particular site. As this procedure was only a practical countermeasure, it was also decided to apply the pressure to the rigid plate up to greater than 400 kPa that was twice of the required value of 200 kPa, to be on the safe side.

Figures 34, 35 and 36 show the results of the SH tests with the NLD interpretation carried out on plates No. 1, No. 2 and No. 3, respectively. Displacements were factored by 1.4 as mentioned previously. It is seen from these figures that displacement on plate No. 2 begins to increase at a loading pressure of 300 kPa while plate No. 1 and No. 3 show linear behaviours up to a pressure of 400 kPa. It is also seen that the stiffness (pressure/displacement) of plate No. 1 is about twice as much as that of plate No. 3.

On the basis of these SH test results, it was able to confirm that all the plates including plate No. 2 have enough capacity larger than the requirement of bearing capacity of 200 kPa.

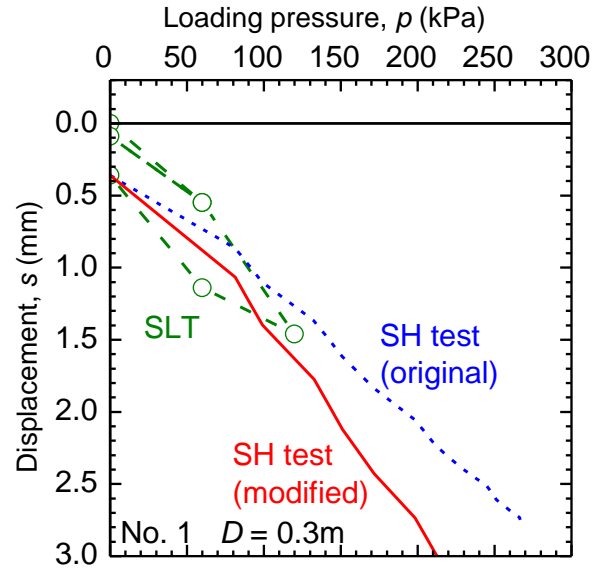


Figure 33 Load-settlement curves of SH test modified

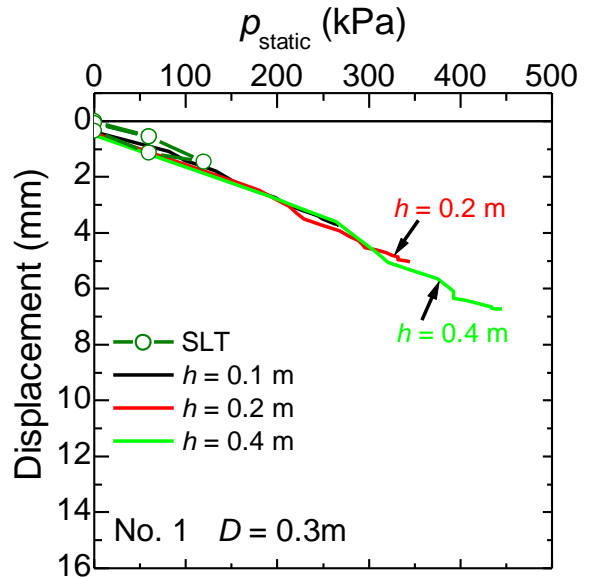


Figure 34 Results of SH tests on plate No. 1

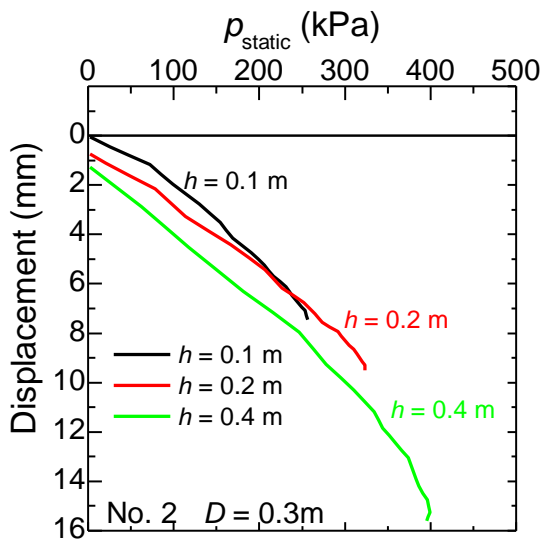


Figure 35 Results of SH tests on plate No. 2

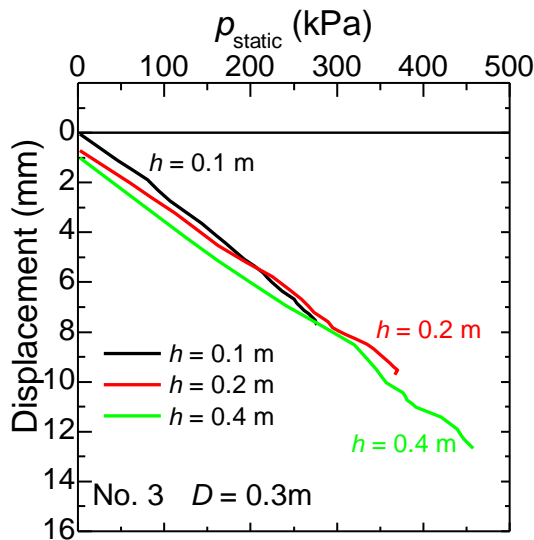


Figure 36 Results of SH tests on plate No. 3

This case study suggests that the static plate load test should be carried out in addition to the SH plate load tests in loam or clay soils where displacements due to consolidation and/or creep may occur, in order to calibrate the SH test results.

Although plate load tests were carried out at only three locations in the site, the test results clearly showed variation of bearing characteristics of the ground. Increase in the number of tests in a site may give us more detail information on the variability of the ground properties. In this aspect, use of the SH test method is promising because of its high mobility. The SH tests and the SLT were completed in a few hours in this site.

### 6.2 Plate Load Test on Improved Soil

Shallow soil improvements are often used for the foundation ground of buildings. It is important to confirm the bearing characteristics of improved soil over the construction area. If the rapid plate load test can be applicable to improved soils, it is one of effective use of the SH test.

A public building of working support facility for handicapped persons was planned to be constructed at the sea side of Tokyo Bay. The foundations of this building consist of PHC piles and partly raft foundation. The top layer is fine sand to a depth of 10 m, underlain

by sandy clay to a depth of 30 m. For the raft foundation, cement-mixing soil improvement was used for the top layer over the construction area. In order to confirm the bearing capacity of the improved ground at the location the raft foundation, a static plate load test was carried out. As the design contact pressure of the raft foundation was 50 kPa, the maximum pressure of 180 kPa was applied in this test. In order to investigate applicability of the SH test on the improved soil, the SH tests were additionally carried out on the same plate one day after the SLT.

Figure 37 shows load-displacement curves from both the SLT and the SH tests. In the SLT, multiple maintained loading was adopted with a load holding time of 30 min for each loading step. As shown in the figure, displacement was generally very small and increase in displacement during load holding was negligible. In the earlier part until an applied pressure of 90 kPa, the inclination of the curve is greater than that in the latter part of loading. This might be attributed to imbibition near the ground surface.

In this site, the results from both SLT and the SH tests show very good agreement because displacement of the improved ground occurs promptly without consolidation and/or creep. For the confirmation of the performance of the improved soil, the SH test can be used as a useful alternative to the static test. Again, it is notable that the SH testing finished in an hour while the SLT required one working day.

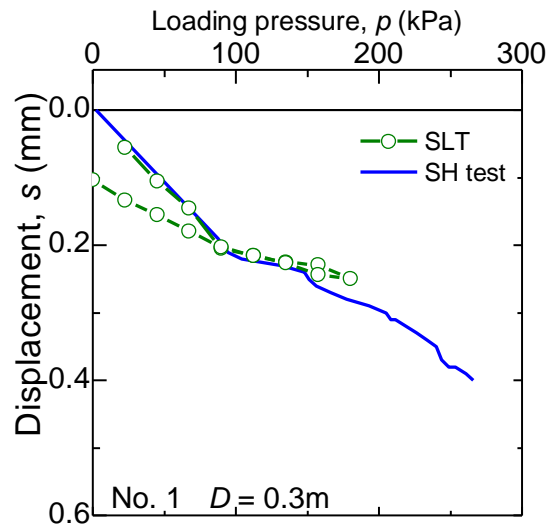


Figure 37 Load-displacement curves obtained from SLT and the SH test on an improved soil

## 7. CONCLUDING REMARKS

As one of rapid load test methods, the Spring Hammer rapid load test method was introduced in this paper.

The validity of the SH test was examined through comparisons of static and rapid load tests. It was shown from the comparative tests that the SH rapid load test with the Non-Linear Damping interpretation method is a good alternatives to the conventional static load test method.

The SH test can be applicable for the rigid plate loading test. However, for the test on the ground where displacement due to the consolidation or creep may occur, calibration using the result of SLT is recommended. On the other hand, the SH test shows good agreement with the result of SLT on a cement-mixing improved ground.

The advantages of the SH tests, such as mobility, quick testing and simple and easy interpretation, enable multiple testing in a site for the estimation of the bearing characteristics over the construction site.

The case studies presented in this paper encourage the use of the Spring Hammer testing for construction and quality controls, and design of foundations.

## 8. REFERENCES

- ASTM (2008). Standard Test Methods for Axial Compressive Force Pulse (Rapid) Testing of Deep Foundations. D 7383 – 8.
- Architectural Institute of Japan (AIJ). (1994). Structural Design and Construction Manual for Temporary Buildings and Structures. pp. 12-15 (in Japanese).
- Bermingham, P. and Janes, M. (1989). An Innovative Approach to Load Testing of High Capacity Piles. Proc. of Int. Conf. on Piling and Deep Foundations, pp. 409-413.
- Gonin, H. G. C. and Leonard, M. S. M. (1984). "Theory and Performance of a New Dynamic Method of Pile Testing", Proc. of 2<sup>nd</sup> Int. Conf. of Application of Stress-Wave Theory to Piles, Stockholm, pp. 403-410.
- Hölscher, P. and van Tol, F. (Edited). (2009). Rapid Load Testing on Piles. CRC Press, UK.
- Japanese Geotechnical Society (2002). Method for Rapid Load Test of Single Piles, JGS 1815-2002, Standards of Japanese Geotechnical Society for Vertical Load Tests of Piles.
- Japanese Geotechnical Society (2003). Standards for Rigid Plate Test, JGS1521-2003.
- Kitiyodom, P., Matsumoto, T. and Kanefusa, N. (2004). Influence of reaction piles on the behaviour of test pile in static load testing. Canadian Geotechnical Journal, June 2004, Vol. 41, No. 3, pp. 408-420.
- Kusakabe, O. and Matsumoto, T. (1995). Statnamic tests of Shonan test program with review of signal interpretation. Proc. 1st Int. Statnamic Seminar, Vancouver, Canada, pp. 13-122.
- Lin, S.S., Hong, J.L. and Lee, W.F. (2004a). Capacity evaluation of Statnamic tested long piles. Soil Dynamics and Earthquake Engineering, Vol. 24, No. 11, pp. 829-838.
- LIN, S.S., HONG, J.L. and LEE, W.F. (2004b). Structural damping concept for interpretation of statnamic pile load test results. GeoSupport 2004, ASCE, GSP No. 124, pp. 169-177.
- Matsumoto, T., Tsuzuki, M. and Michi, Y. (1994). Comparative Study of Static Loading Test and Statnamic on A Steel Pipe Pile Driven in A Soft Rock. Proc. of 5th Int. conf. and Exhibition on Piling and Deep Foundations, Bruges, Belgium, pp. 5.3.1 - 5.3.7.
- Matsumoto, T., Wakisaka, T., Wang, F. W., Takeda, K. and Yabuuchi, N. (2004). Development of a rapid pile load test method using a falling mass attached with spring and damper. Proc. 7th Int. Conf. on the Appl. of Stress-Wave Theory to Piles, Selangor, Malaysia, pp. 351-358.
- Matsuzawa, K., Nakashima, Y. and Matsumoto, T. (2008a). Spring Hammer Rapid Load Test and Its Validations. Proc. of 2<sup>nd</sup> Int. Conf. on Foundations, Dundee, Scotland, pp. 223-234.
- Matsuzawa, K., Nakashima, Y., Nakayama, M. and Matsumoto, T. (2008b). A piling method accompanying rapid load testing, Proc. 8th Int. Conf. on Appl. of Stress-Wave Theory to Piles, Lisbon, Portugal, pp. 487-495.
- Middendorp, P., Bermingham, P. and Kuiper, B. (1992). Statnamic loading testing of foundation piles. Proc. of 3rd Int. Conf. of Appl. of Stress-Wave Theory to Piles, The Hague, Netherlands, pp. 581-588.
- MULLINS, G., LEWIS, C. and Justason, M. (2002). Advancements in statnamic data regression technique. Deep Foundations 2002, ASCE, Vol. 2, GSP No. 116, pp. 915-930.
- Poulos, H.G. (1998). Pile testing - From the designer's viewpoint. Proc. of 2nd Int. Statnamic Seminar (edit. Kusakabe, Kuwabara & Matsumoto), Tokyo, pp. 3-21.
- Randolph, M. F. and Deeks, A. J. (1992). "Dynamic and Static Soil Models for Axial Pile Response", Proc. 4<sup>th</sup> Int. Conf. on Appl. of Stress-Wave Theory to Piles, Hague, pp.3-14.
- Raushe, F., Goble, G. and Likins, G. E., Jr. (1985). Dynamic determination of pile capacity. J. Geotech. Div., ASCE, Vol. 111, No. 3, pp. 367-383.
- Schellingerhout, A. J. G., and Revoort, E. (1996). Pseudo Static Pile Load Tester. Proc. of 5<sup>th</sup> Int. Conf. on Application of Stress-Wave Theory to Piles, Orland, pp. 1031-1037.
- Stokes M, Mullins, G., Ealy, C., and Winters D. (2008) Statnamic damping coefficient: Numerical modeling approach, Journal of Geotechnical and Geoenvironmental Engineering, ASCE, vol. 134, No. 9, pp. 290-1298.